



27th International Conference on Flexible Automation and Intelligent Manufacturing, FAIM2017,
27-30 June 2017, Modena, Italy

Robotic AM system for plastic materials: tuning and on-line adjustment of process parameters

Paolo Magnoni^{a,b,*}, Lara Rebaioli^{a,*}, Irene Fassi^a, Nicola Pedrocchi^a,
Lorenzo Molinari Tosatti^a

^aConsiglio Nazionale delle Ricerche, Institute of Industrial Technologies and Automation, via A. Corti 12, 20133 Milan, Italy

^bUniversity of Brescia, Dep. of Mechanical and Industrial Engineering, via Branze 39, 25123 Brescia, Italy

Abstract

Additive Manufacturing (AM) techniques based on thermoplastic polymer extrusion allow the manufacture of complex parts, but their slow printing speed limits their use for mass production. To overcome this drawback, an industrial screw-based extruder has been mounted on an anthropomorphic robot, realizing a flexible AM platform for big objects. The most important process parameters have been set by a suitable experimental campaign, ensuring a regular deposited layer geometry. A closed-loop control has been implemented to further improve the process parameter setting based on data measured during the deposition, in this way compensating the material withdrawal or other unexpected defects.

© 2017 The Authors. Published by Elsevier B.V. This is an open access article under the CC BY-NC-ND license (<http://creativecommons.org/licenses/by-nc-nd/4.0/>).

Peer-review under responsibility of the scientific committee of the 27th International Conference on Flexible Automation and Intelligent Manufacturing

Keywords: Additive Manufacturing (AM); Fused Deposition Modeling (FDM); Industrial robotics; Process parameters tuning; Deposition process monitoring; Design of Experiments.

* Corresponding authors.

E-mail addresses: paolo.magnoni@itia.cnr.it; lara.rebaioli@itia.cnr.it

1. Introduction

The use of Additive Manufacturing (AM) techniques based on the extrusion of thermoplastic polymers, such as Fused Deposition Modeling (FDM) [1], has increased significantly in recent years [2]. Although AM allows the manufacture of customized and complex parts, the slow printing speed of standard AM systems limits their use for mass production. For this reason, a productivity improvement and an increment of achievable part size are key targets for future manufacturing systems [3]. Industrial extruders mounted on robotic manipulators allow a fused material deposition rate that is 10 to 20 times higher than the average deposition rate of commercial FDM systems. Moreover, AM system based on robotic platforms could replace some of the application functions of FDM printers providing more flexibility, better motion software support and an industrial level of reliability [4]. Eventually, the use of plastic pellets instead of wires results in a cost reduction and a higher freedom in material selection.

Despite of these advantages, there are some drawbacks related to the manufacturing of big parts with high deposition rates, such as the irregular shape of deposited material in case of non-optimally tuned process parameters, which results in geometrical errors on the final part. Another critical issue is the material withdrawal during the cooling phase, which could modify the deposited layer geometry.

In the present study, an industrial screw-based extruder has been modified and mounted on an anthropomorphic robot, realizing a flexible platform for the additive manufacturing of big objects. This work addresses the aforementioned limitations proposing a method to find optimal values for relevant process parameters (Section 3) and a method for online monitoring and control of process state-variables, thanks to the integration of sensors into the robotic system (Section 4). The values of process parameters (i.e. extruder motor rotational speed, robot translation speed, nominal layer height) are found by performing a campaign of 81 experiments on single-layer rectilinear tracks based on a suitable experimental design, which has been developed according to Design of Experiments (DoE). Subsequently, the refinement of the parameter values and their correction when depositing many layers can be done thanks to a discrete control law based on the sensor measurements during the deposition. The effectiveness of the proposed procedure is demonstrated by a representative case study of additive manufacturing of big parts, i.e. a piece of furniture (Section 5).

1.1. State-of-the-Art and Related Works

There are only few examples of state-of-the-art systems able to manufacture plastic parts with deposition rates more than 20 times higher than standard high-end 3D printers [5]. In particular, the Oak-Ridge-National-Laboratory in collaboration with Cincinnati Inc., developed a BAAM (Big Area Additive Manufacturing) system able to deposit with a 15000 cm³/h flow rate [6]. The problems of extensive warping due to material withdrawal and irregular shape of deposition have been solved adding carbon fibers to the extruded material and including a mechanical compactor in the extruder design [5]. In that case, the extruder was integrated with a gantry-style robotic automation cell, but other examples of commercial setups for robotized AM use anthropomorphic robots [7,8]. However, none of the aforementioned systems presents a detailed discussion of the procedure to find printing parameters or includes control loops during the deposition process.

The existing literature on the estimation of optimal deposition parameters focuses on standard 3D printing and not on BAAM. In a work by Sood [9], the influence of processing parameters such as layer thickness, orientation, raster angle, raster width and air gap is studied. These parameters can change the dimensional accuracy, the surface roughness and the mechanical properties of the printed part. However, this study assumes that each deposited track is regular thanks to consolidated use of PLA and ABS in standard 3D printing machines. This assumption can be found in other works [10-12]. This is no longer true with a large deposition rate and, as a consequence, this study will focus on the basic parameters able to guarantee a regular deposition of each plastic track: rotational speed of the extruder motor, translation speed of the robot, nominal layer height commanded to the robot.

Concerning the process monitoring in order to achieve a better deposition, many works about the monitoring of laser-based AM processes can be found in literature. Mazumder [13] resumes the state-of-art. Fewer works are focused on the monitoring of plastic deposition processes: Dinwiddie [14,15] measures the temperature of the deposited material, and Faes [16] describes a laser scanner able to recognize the shape of the tracks extruded by a standard 3D printer. However, most FDM machines lack every sort of feedback yet. Possible causes are: (i) the

relative stability of FDM process for standard deposition rates (e. g., using traditional nozzle diameter values) does not require a feedback control; (ii) 3D printers and CNC machines are harder to be augmented with a control loop than robot controllers where multi-threading can be exploited; (iii) implementing a feedback control would increase the relatively low cost of such systems.

Nomenclature

e_k	Error between $\Delta x_{ref,k}$ and $\Delta \tilde{x}_{mean,k}$
v_t	Robot translation speed
w_{mean}	Measured mean layer width
β	Overlap factor
$\Delta x_{ref,k}$	Nominal layer height (k^{th} layer) with an additional height to guarantee an overlap between layers
$\Delta \tilde{x}_{mean,k}$	Measured mean layer height (k^{th} layer) with an additional height to guarantee an overlap between layers
Δz_{diff}	Difference between nominal and measured mean layer height
Δz_{mean}	Measured mean layer height
$\Delta z_{ref,k}$	Nominal layer height (k^{th} layer)
λ	Proportional gain in the control law
ω_m	Extruder motor rotational speed

2. Setup description

The setup is composed by a 6-axes ABB IRB-2600 anthropomorphic robot (20 kg of payload, 1.65 m of reachability) equipped with a single screw Gimac industrial extruder. The extruder derives from the “microextruders” family of Gimac products and it has a pellet feeding system (hopper), four heated zones and a conic deposition nozzle (with a \varnothing 2 mm hole). The system is equipped with a laser triangulation sensor (Fig. 1b) to measure distances within the measurement range of $50 \text{ mm} \pm 10 \text{ mm}$ and a resolution up to $2 \text{ }\mu\text{m}$. A $80 \times 80 \text{ mm}$ heated bed can guarantee an adequate adhesion with many different materials.

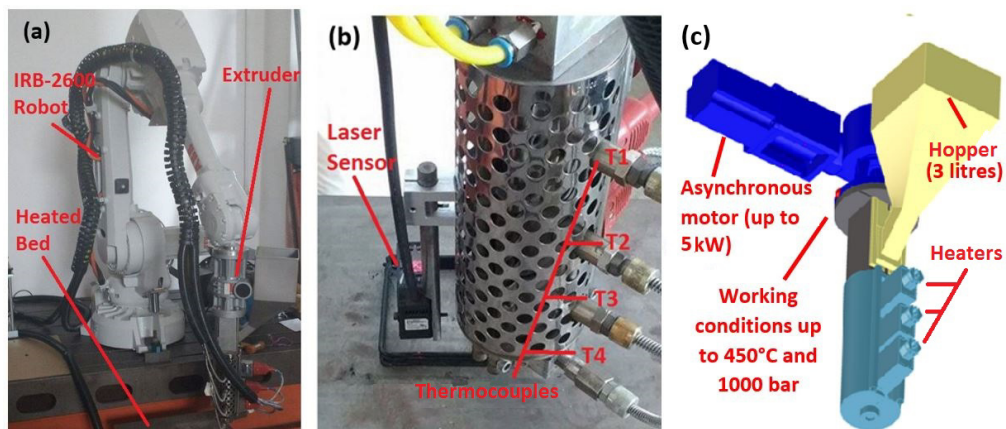


Fig. 1. (a) Robotic system to print big parts with plastic materials, developed by CNR-ITIA with the collaboration of Gimac S.r.l.; (b) Laser measurement sensor attached on the extrusion head; (c) Scheme of the extruder.

3. Process parameter tuning

3.1. Objectives and definitions

In the process parameter tuning phase, a suitable experimental campaign has been developed according to a DoE to set the most important process parameters (extruder motor rotational speed, robot translation speed, nominal layer height) ensuring a regular and constant geometry of the deposited layer. In addition, this experimental design allows to identify the relationship between the process parameters and the deposited track height and width.

For the whole experimental work, the selected target material is PLA (NatureWorks Ingeo™ Biopolymer 4043D) that is the most common material in conventional FDM. A specific black colorant additive is combined with PLA directly in the extruder hopper, to make the material visible by the laser measurement sensor (Section 2).

In this experimental campaign, the simplest possible geometry has been considered and single-layer rectilinear tracks have been deposited keeping constant the parameters listed in Table 1. Based on preliminary experiments, the selected temperatures of the four heating zones (Fig. 1b) are the lowest temperatures allowing the material deposition, thus implying a quick solidification.

After cooling, the track height and width have been measured by a micrometer caliper, taking 5 equally-spaced measurements along each track.

Table 1. Constant parameters for track deposition experiments.

Factor	Value
Track length	200 mm
Number of layers	1
Temperature – extruder zone 1 (T_1)	156°C
Temperature – extruder zone 2 (T_2)	164°C
Temperature – extruder zone 3 (T_3)	155°C
Temperature – extruder zone 4 (T_4)	147°C
Temperature – heated bed	88°C

Table 2. Experimental design summary.

Factor	Symbol	Levels
Extruder motor rotational speed	ω_m	400, 650, 900 rpm
Robot translation speed	v_t	15, 20, 25 mm/s
Nominal layer height	Δz_{ref}	1.5, 2, 2.5 mm

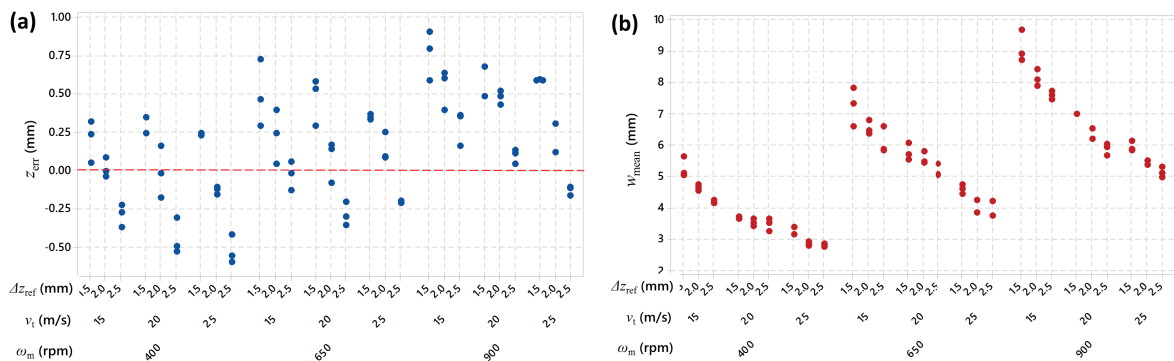


Fig. 2. (a) Individual value plot of mean height difference (Δz_{diff}); (b) Individual value plot of mean width (W_{mean}).

3.2. Method and experimental design

A proper full factorial experimental design, summarized in Table 2, has been studied to point out the effects of the three selected process parameters (extruder motor rotational speed, robot translation speed, nominal layer height) on the deposited layer geometry. Each factor has three levels (whose values have been selected based on preliminary

experiments) and each one of the $3^3 = 27$ experimental conditions has been replicated three times, thus the whole experimental design has consisted of 81 runs, which have been completely randomized.

The experimental responses are the mean height (Δz_{mean}) and width (w_{mean}) of the track, calculated as the mean of the five measured values. The difference between the nominal layer height and the measured mean height is calculated as follows:

$$\Delta z_{\text{diff}} = \Delta z_{\text{ref}} - \Delta z_{\text{mean}} \quad (1)$$

3.3. Results

Fig. 2 shows the experimental results in terms of track height difference (Δz_{diff}) and mean width (w_{mean}). It should be noted that some experimental conditions ($\omega_m = 400$ rpm, $v_t = 25$ mm/s, $\Delta z_{\text{ref}} = 2.0$ mm and $\omega_m = 400$ rpm, $v_t = 25$ mm/s, $\Delta z_{\text{ref}} = 2.5$ mm) resulted in tracks that were similar to undeformed filaments, just deposited on the heated table. Such layers are detrimental from the manufacturing point of view, thus these experimental conditions correspond to unsuitable process parameter combinations.

A linear regression analysis has been performed to describe the relationship between the process parameters and the track height difference and mean width. The regression analysis shows how all factors and some interactions between them influence both the responses. The main results of the regression analysis (p-values and estimated standard deviation) are summarized in Table 3 while the estimated regression models (uncoded predictors) of the two responses are expressed by Equations (2) and (3) (terms in square brackets refer to not significant factors that are left in the model for the sake of hierarchical completeness). The adequacy of the regression models is demonstrated by the coefficient of determination (R^2_{adj}) high values, which are 89.93 % and 97.28 %, respectively, and by the high p-values of the lack of fit test, which are 0.632 and 0.144, respectively.

$$\Delta z_{\text{diff}} = -0.107 + 0.0017 \cdot \omega_m + 0.0444 \cdot v_t \left[-0.236 \cdot \Delta z_{\text{ref}} \right] - 0.00004 \cdot (\omega_m \cdot v_t) - 0.01916 \cdot (v_t \cdot \Delta z_{\text{ref}}) \quad (2)$$

$$w_{\text{mean}} = 8.10 + 0.0172 \cdot \omega_m - 0.580 \cdot v_t - 1.390 \cdot \Delta z_{\text{ref}} - 0.00021 \cdot (\omega_m \cdot v_t) - 0.0012 \cdot (\omega_m \cdot \Delta z_{\text{ref}}) + 0.0661 \cdot (v_t \cdot \Delta z_{\text{ref}}) - 0.000004 \cdot (\omega_m)^2 + 0.0088 \cdot (v_t)^2 \quad (3)$$

Table 3. Regression analysis p-values ($\alpha = 1\%$, bold: significant factors, italic: nearly significant factor) and estimated standard deviation.

	ω_m	v_t	Δz_{ref}	$\omega_m \cdot v_t$	$\omega_m \cdot \Delta z_{\text{ref}}$	$v_t \cdot \Delta z_{\text{ref}}$	ω_m^2	v_t^2	estimated standard deviation (mm)
Δz_{diff}	0.000	<i>0.020</i>	0.128	<i>0.013</i>	<i>0.014</i>	---	---	---	0.1103
w_{mean}	0.000	0.000	0.003	0.000	0.002	0.001	0.001	0.001	0.2704

Except for the aforementioned unsuitable combinations of process parameters, all the other process parameter sets can be selected. Equation (2) can be used to find a process parameter combination that guarantees a null (or nearly null) height difference (Δz_{diff}), meaning that the extruder motor rotational speed and the translation speed give an appropriate throughput for the layer height set in the robot motion control. For example, if high levels of extruder motor rotational speed and robot translation speed are selected to achieve the highest productivity, Equation (2) provides the suitable value of nominal layer height. Subsequently, Equation (3) can be used to estimate the track mean width for the selected process parameter combination. The resulting nominal layer height and track width values represent the input for the slicing software that produces the part program for complex objects.

4. Process parameters on-line adjustment

When realizing multi-layer objects, layer deformation can occur due to the pressure of successive layers on the previously deposited ones and due to material withdrawal. As a consequence, even with fixed extruder motor

rotational speed and robot translation speed, the actual layer height can become different from the nominal layer height (“commanded robot height”). In particular, an actual layer height that is too low (Fig. 3) or too high (Fig. 4) can determine deformations in the obtained object. As a consequence, a control strategy has been implemented to maintain deviations in layer height and width within a tolerance range. Moreover, this control strategy can lead to the convergence towards optimal process parameters also in the case that a complete process parameter tuning (Section 3) cannot be performed.



Fig. 3. Robot height **above** the optimal range: (a) Scheme of the effect caused by a too high commanded robot height; (b) Deposition defects in a real experiment using square geometry; (c) Deposition defect measured with laser sensor as error between nominal and measured layer height.

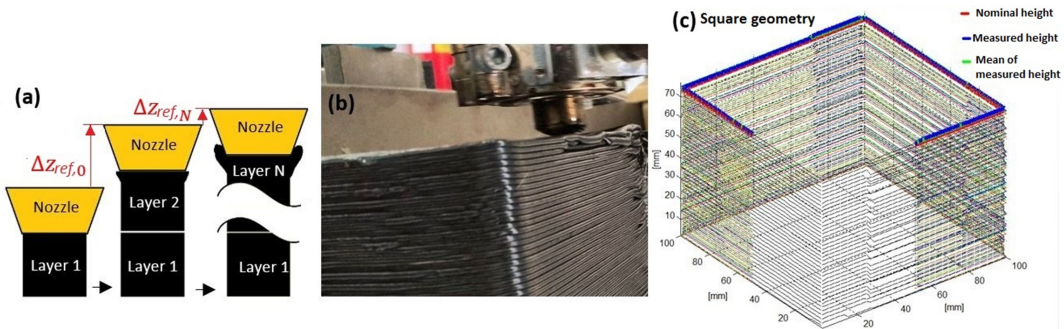


Fig. 4. Robot height **under** the optimal range: (a) Scheme of the effect caused by a too low commanded robot height; (b) Deposition defects in a real experiment using square geometry; (c) Deposition defect measured with laser sensor as error between nominal and measured layer height.

4.1. Method

Once the deposition of each layer has been performed, the robot positions itself at a height where the sensor can measure distances without a contact between the material and the nozzle. Then, the robot moves again along the underlying layer path, activating the measurement procedure. It is possible to store a measure from the laser sensor every 1 mm of robot translation (blue line in Fig. 3c and 4c) and compute the mean for each layer actual height (green line in Fig. 3c and 4c). If the measured mean height is bigger than the nominal one (red line in Fig. 4c), it means that an excessive pushing on the solidifying material will happen when depositing upper layers. This causes an accumulation of material that changes the width of each track and compromises the object fabrication, worsening layer after layer. If the measured height is smaller than the nominal one (red line in Fig. 3c), it means that no adequate pressure is applied when depositing upper tracks, with a subsequent weak welding between layers. Moreover, in this case, the commanded robot height can accumulate error causing the material falling from the nozzle without any contact. A correct contact is guaranteed by an overlap (β) between each track and the upper one. A good overlap value can be estimated as the 20% - 30% of the commanded robot height.

To guarantee this correct overlap and prevent a commanded robot height that is too high or too low, it is possible to implement a control strategy. Possible strategies can modulate the extruder motor speed or modify the robot commanded height. In this work, the latter approach is adopted, improving the regularity of deposited layers, although modifying the final height of the object.

The correction strategy can be explained as follows:

- Given a starting set of parameters ω_m , v_t , $\Delta z_{ref,0}$, the ideal height of the deposited material can be written as $\Delta x_{ref,0}$ that is higher than $\Delta z_{ref,0}$ to allow the desired overlap β : $\Delta x_{ref,0} = (1 + \beta)\Delta z_{ref,0}$ with $\beta \in [0.2-0.3]$.
- If we denote the mean of the measured material height as $\Delta \tilde{x}_{mean,0}$, the error between the nominal material height and the measured one can be written as $e_0 = \Delta \tilde{x}_{mean,0} - \Delta x_{ref,0}$. As a consequence, a simple proportional control algorithm at the k_{th} layer can be written as:

$$\Delta z_{ref,k+1} = \Delta z_{ref,k} + \lambda(e_k) = \Delta z_{ref,k} + \lambda(\Delta \tilde{x}_{mean,k} - \Delta x_{ref,k}) = \Delta z_{ref,k} + \lambda(\Delta \tilde{x}_{mean,k} - (1 + \beta)\Delta z_{ref,k}) ; \forall k = 0 \dots N-1 \quad (4)$$

This imply that the robot trajectory is modified with the computed height $\Delta z_{ref,k+1}$ that can minimize the error with a correct gain $\lambda < 1/(1 + \beta)$ able to guarantee a proper convergence.

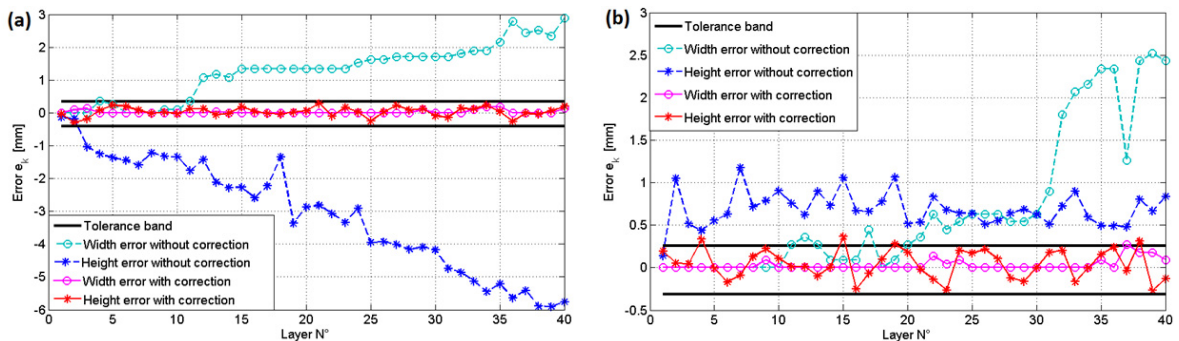


Fig. 5. Dimensional errors (mean layer height error and mean layer width error) measured in correspondence of each layer of a real experiment using a square geometry: (a) Error caused by robot height 15% above the optimal range and its correction using the control strategy; (b) Error caused by robot height 15% under the optimal range and its correction using the control strategy.

4.2. Results

To demonstrate the effectiveness of the proposed correction algorithm, two tests have been performed starting from an optimal value of $\Delta z_{ref,0}$, i.e. 2.2 mm. This value is in the centre of the operative range described in Section 3 and it allows a regular behavior and little errors for many layers. Fig. 5a shows the improvements achievable if using the control algorithm in case of a $\Delta z_{ref,0}$ value which is too high (15% higher than the optimal value or in case of

underlying material shrinkage). Without the correction algorithm, the mean layer height error $e_k = \Delta \tilde{x}_{mean,k} - \Delta x_{ref,k}$ ($\forall k = 0 \dots N-1$) increases, and also the mean layer width error increases because of the material falling and creating curls or irregular rods. Thanks to the adaptation of robot height according to Equation (4), it is possible to maintain the shape under control and within a tolerance interval. Analogue improvements can be achieved in case of starting commanded robot height 15% lower than the optimal value of 2.2 mm (Fig. 5b).

5. Case study and conclusions

As a case study, a piece of furniture has been realized using the considered setup running with the process parameters found in Section 3 ($\omega_m = 650$ rpm, $v_t = 25$ mm/s, $\Delta z_{ref} = 2.2$ mm, extruder temperature range = 147 °C - 164°C, heated bed temperature = 88°C). With these parameters, the system has a deposition flow rate of about 1250 cm³/h and it is able to produce the chair in Fig. 6a in about 6 hours using colored PLA. The trajectory has been

generated thanks to a custom version of the Slic3r© [17] software, able to act as a CAD/CAM software for the considered system and to generate a part program containing the motion instructions for both the robot and the extruder. The layer height control of Section 4 has also been included into the part program: a measure with the laser sensor has been performed every 10 layers, observing that the starting parameters led to an accumulation of material. As a consequence, the commanded robot height has been automatically and gradually increased, resulting in total correction of +8 mm. This implies that the resulting chair is 8 mm higher than the original CAD file, but the use of the layer height control guarantees a constant shape of the deposited tracks and, therefore, a successful manufacturing of complex geometries as the one presented in this section. Future works on online re-slicing according to layer height monitoring will be able to preserve the original CAD height while maintaining the optimal overlap between layers.

The case study demonstrated the effectiveness of the approach presented in this paper, which is composed by the following steps: (i) an experimental campaign designed according to DoE, in order to find a suitable range of process parameters; (ii) a closed loop control strategy able to correct the robot height, in order to guarantee a regular shape of deposited *tracks* for each layer.

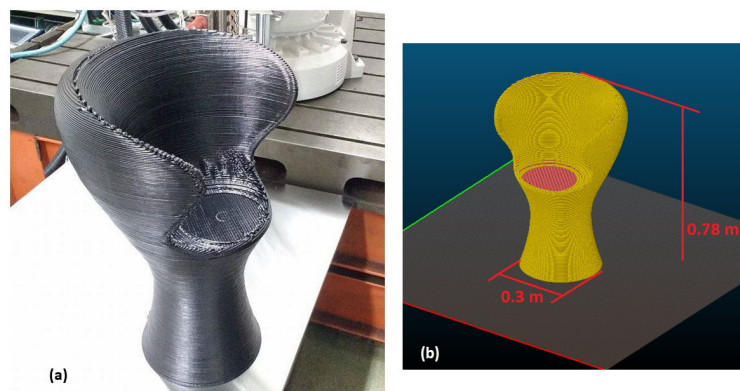


Fig. 6. (a) Final example of an object obtained with the described setup: armchair made using PLA mixed with black colorant; (b) CAD file of the printed chair visualized using the slic3r© software and with the object size.

Acknowledgements

The described setup has been developed in collaboration with Gimac International S.r.l., which realized the industrial extruder. We also would like to thank ABB Robotics Italy for the support.

References

- [1] I. Gibson, D. Rosen, B. Stucker, Additive Manufacturing Technologies: 3D Printing, Rapid Prototyping and Direct Digital Manufacturing, Springer, New York, 2010.
- [2] T. Wohlers, T. Caffrey, Wohlers report 2015: 3D printing and additive manufacturing state of the industry annual worldwide progress report, Wohlers Associates, 2015.
- [3] N. Guo, M. C. Leu, Front. Mech. Eng. 8 (2013) 215-243.
- [4] G. Q. Zhang, X. Li, R. Boca, J. Newkirk, B. Zhang, T. Fuhlbrigge, H. Feng, N. Hunt, Use of Industrial Robots in Additive Manufacturing - A Survey and Feasibility Study, Conference ISR ROBOTIK, Berlin, 2014.
- [5] S. S. Babu, L. Love, R. Dehoff, W. Peter, T. R. Watkins, S. Pannala, MRS Bull., 40 (2015) 1154-1161.
- [6] «BAAM (Big Area Additive Manufacturing)» [Online]. Available: <http://web.ornl.gov/sci/manufacturing/>. [Last accessed on 01-2017].
- [7] «Branch Technology» [Online]. Available: <http://www.branch.technology/>. [Last accessed on 01-2017].
- [8] «Stratasys Robotic AM» [Online]. Available: <http://blog.stratasys.com/2016/08/24/infinite-build-robotic-composite-3d-demonstrator/>. [Last accessed on 01-2017].
- [9] A. K. Sood, Study on parametric optimization of fused deposition modelling (FDM) process, PhD thesis, National Institute of Technology Rourkela, 2011.

- [10] M. Montero, S. Roundy, D. Odell, S.-H. Ahn, P. K. Wright, Material characterization of fused deposition modeling (FDM) by designed experiments, Proceedings of Rapid Prototyping and Manufacturing Conference, SME, (2001) 1-21.
- [11] R. Anitha, S. Arunachalam, P. Radhakrishnan, . Mater. Process. Technol. 118 (2001) 385-388.
- [12] Y. Zhang, K. Chou, Proc. Inst. Mech. Eng. Part B-J. Eng. Manuf. 222 (2008) 959-968.
- [13] J. Mazumder, D. Dutta, N. Kikuchi, A. Ghosh, Opt. Lasers Eng. 34 (2000) 397-414.
- [14] R. B. Dinwiddie, L. J. Love, J. C. Rowe, Realtime process monitoring and temperature mapping of a 3D polymer printing process, SPIE Defense, Security, and Sensing. International Society for Optics and Photonics., (2013) 1-9.
- [15] R. B. Dinwiddie, V. Kunc, J. M. Lindal, B. Post, R. Smith, L. Love, C. Duty, Infrared imaging of the polymer 3D-printing process, SPIE Sensing Technology Applications. International Society for Optics and Photonics, (2014) 1-12.
- [16] M. Faes, W. Abbeoos, F. Vogeler, H. Valkenaers, K. Coppens, E. Ferraris, Process monitoring of extrusion based 3D printing via laser scanning, PMI 2014 Conference Proceedings, 6 (2014) 63-67.
- [17] «Slic3r open source software» [Online]. Available: <http://slic3r.org/>. [Last accessed on 04-2017].